DOI:, available online at www.cjmenet.com; www.cjmenet.com.cn

Kinematic Calibration and Forecast Error Compensation of a 2-DOF Planar Parallel Manipulator

CHANG Peng[1,*], LI Chengrong[1], and LI Tiemin[2]

1 *Hi-tech Innovation Center, Institute of Automation Chinese Academy of Sciences, Beijing 100190, China*
2 *Department of Precision Instruments and Mechanology, Tsinghua University, Beijing 100084, China*

Received January 28, 2010; revised December 17, 2010; accepted **, 2011; published electronically **, 2011

Abstract: This paper presents a method combined step kinematic calibration and linear forecast real-time error compensation in order to enhance the precision of a two degree-of-freedom (DOF) planar parallel manipulator of a hybrid machine tool. Due to large workspace, heavy-duty and over-constrained mechanism, a small deformation is caused and the precision of the 2-DOF planar parallel manipulator is affected. The kinematic calibration cannot compensate the end-effector errors caused by the small deformation. In the step kinematic calibration phase of the method, the end-effector errors caused by the errors of major constant geometrical parameters is compensated. The step kinematic calibration is based on the minimal linear combinations (MLCs) of the error parameters. All simple and feasible measurements in practice are given, and identification analysis of the set of the MLCs for each measurement is carried out. According to identification analysis results, both measurement costs and observability are considered, and a step calibration including step measurement, step identification and step error compensation is determined. The linear forecast real-time error compensation is used to compensate the end-effector errors caused by other parameters after the step kinematic calibration. Taking the advantages of the step kinematic calibration and the linear forecast real-time error compensation, a method for improving the precision of the 2-DOF planar parallel manipulator is developed. Experiment results show that the proposed method is robust and effective, so that the position errors are kept to the same order of the measurement noise. The presented method is attractive for the 2-DOF planar parallel manipulator and can be also applied to other parallel manipulators with fewer than six DOFs.

Key words: parallel manipulator, kinematic calibration, error compensation, minimal linear combinations (MLCs)

1 Introduction

Calibration is vitally important to any computer-controlled parallel manipulator when high precision is required. An accurate mathematical model is essential for a machine to achieve excellent positioning performances. However, the actual system parameters inevitably deviate from their nominal values due to manufacture and assembly errors. Thus the accuracy of a manipulator is limited. Kinematic calibration gives an available and effective solution method [1]. It is a process by which the accuracy of a parallel manipulator can be improved by modifying the control software rather than changing or altering the design of the machine[2]. There are four sequential steps in a calibration process, including modeling, measurement, identification and error compensation[3].

But kinematic calibration has its limitations[4-5]: the simplified model in calibration doesnot include all the kinematic parameters of parallel manipulators; the measurable workspace is small because of the restricted motion pattern of the parallel manipulators; kinematic parameters of individual links are computed separately, therefore, the coupling effects among the legs are not fully explored. In calibration model, the major constant geometrical parameters can be considered, and the other parameters (for example, variable parameters and minor kinematic parameters) are ignored. The limitations become apparent in the kinematic calibration for parallel manipulators with large workspace, heavy-duty and over-constrained mechanism. In order to overcome the limitations, complicated models or assistant methods are developed[6-8].

Huang and Tang[9] reported a hierarchical approach to the geometric error identification by means of the characteristic that a 3 degree-of-freedom (DOF) milling machine pose errors can be separated. Chang and Li[10] stated that the manipulator kinematics was uniquely determined by a set of minimal parameters which are in fact the linear combinations of the original error parameters and are linearly independent. These parameters are termed the minimal linear combinations (MLCs) of the error parameters in the context. Since obtaining the MLCs will

* Corresponding author. E-mail: changpeng@tsinghua.org.cn
This project is supported by National Natural Science Foundation of China (Grant No. 50805140), and National Hi-tech Research and Development Program of China(863 Program, Grant No. 2007AA04Z227)

facilitate solving the parameter identification problem, they introduced four demonstrated theorems to find the sets of the MLCs.

This paper presents a method combined step kinematic calibration based on the MLCs and linear forecast real-time error compensation for a 2-DOF planar parallel manipulator. Four theorems are used to find the different sets of the MLCs in identification analysis of each relative measurement (RM), and avoid the influence of irrespective parameters. The step measurement, step identification and step error compensation are then determined considering both the measurement costs and the observability. The step kinematic calibration can enhance the precision of identification in each step, and eliminate the end-effector errors due to the major constant geometrical parameters errors. But other parameters (for example, variable parameters) affect the end-effector positioning accuracy to a certain extent in the 2-DOF planar parallel manipulator with large working space, heavy-duty and over-constrained mechanism. The variable parameters are generated by the small distortions of geometrical parameters by gravity and over-constrained mechanism. After the step kinematic calibration, the linear forecast real-time error compensation is used to compensate the end-effector errors caused by other parameters. Experiment results show that the proposed method is simple, effective and easy to implement, so that the errors in position are kept to the same order of the measurement noise.

In this paper, section 2 describes the 2-DOF planar parallel manipulator under consideration, and the step kinematic calibration is presented: kinematic error model, identification analysis based on the MLCs in different measurements, step measurement and step error compensation. The linear forecast real-time error compensation is discussed in section 3. Experiment results are reported in section 4. Finally, section 5 gives the conclusions.

2 Kinematic Calibration

2.1 Structure description

In order to mill huge blades and guide vanes of hydraulic or steam turbines, a duty hybrid machine tool with 5 DOFs is designed. Due to the large volume, the machine stiffness will be low if it is designed as the conventional serial structure. Thus, a 2-DOF parallel manipulator is adopted. Combining the parallel manipulator with a feed worktable and a 2-DOF rotational milling head, a heavy duty hybrid machine tool with 5-DOF is created. The machine tool is designed as 21 m×7.2 m×8.72 m in length (worktable feeding direction), width and height, respectively, and it is usually used to carry out 5-face milling. Furthermore, two additional milling heads without rotational capability are designed to replace the 2-DOF milling head and can be mounted on the side or underside of the moving platform. At this time the heavy duty machine tool can be capable of 3-axis machining vertically or horizontally[11].

The parallel manipulator is composed of a gantry frame, a moving platform, and four length-fixed struts, as shown in Fig.1. Two parallelogram mechanisms are formed on both side of the platform. Two sliders, which are attached to the guideways by prismatic joints and connected to the platform by two parallelogram mechanisms, drive the platform when they slide along the vertical guideways. Thus, the moving platform possesses a 2-DOF purely translational moving capability in a plane. The whole construction enables movement of the moving platform in two directions (*y*- and *z*- axes).

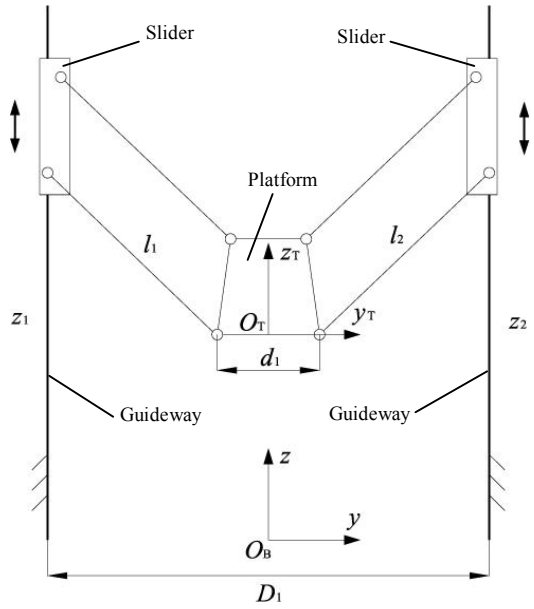

Fig. 1. Structure sketch of the parallel manipulator

2.2 Kinematic error model

The simplification is carried to the point where the kinematic model is amenable to mathematical treatment: two top length-fixed struts on both side of the platform are eliminated, the two residual bottom length-fixed struts, the guideways and the sliders are translated to the centre of platform, and let the end-effector be with the constant-orientation of zero.

Since the kinematic model in the present numerical control system only considers the manipulator motion in a plane, the error along the *x*-axis cannot be compensated. In this paper, we consider only the kinematic error model in the $O_B - yz$ plane. As shown in Fig. 2, the base coordinate frame $O_B - yz$ is set on the worktable with its origin at the midpoint of D, the *y*- and *z*-axes along horizontal and vertical lines, respectively. The two struts are connected to the sliders and the platform with revolute joints O_T, $T_1 \sim T_2$. Parameters l_i ($i = 1,2$) are the lengths of legs, respectively. D is the distance between the two guideways. z_1 and z_2 denote the displacements of sliders from *y*-axis. The origin of the mobile coordinate frame on $O_T - y_T z_T$ platform is at O_T, and z_T-axis lies

along the tool center line. β_1 and β_2 denote, respectively, the angles between vertical line and two orientations of the guideways. $\boldsymbol{n}_1$ and $\boldsymbol{n}_2$ are, respectively, the unit direction vectors of $l_1\boldsymbol{n}_1$ and $l_2\boldsymbol{n}_2$. The values of the nominal parameters in the parallel manipulator are given as $D = D_1 - d_1 = 3\,584$ mm, $l_1 = l_2 = 3\,350$ mm, $\beta_1 = \beta_2 = 0$ rad.

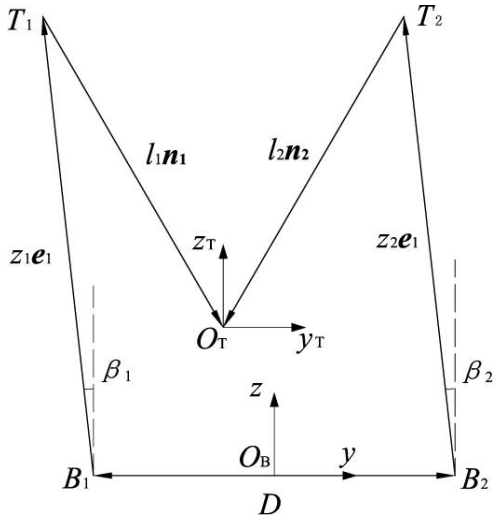

Fig. 2. Vector chain of the parallel manipulator with error parameters

The pose of the platform can be expressed by a vector

$$\boldsymbol{X} = (y \;\; z)^{\mathrm{T}}. \tag{1}$$

From the base coordinate frame $O_{\mathrm{B}} - yz$ to the mobile coordinate frame $O_{\mathrm{T}} - y_{\mathrm{T}}z_{\mathrm{T}}$, there are two closed chains $O_{\mathrm{B}} - B_1 - T_1 - O_{\mathrm{T}}$ and $O_{\mathrm{B}} - B_2 - T_2 - O_{\mathrm{T}}$, which can be established by the following equations

$$\boldsymbol{X} = \boldsymbol{B}_1 + \boldsymbol{R}_{\beta 1} z_1 \boldsymbol{e}_1 + l_1 \boldsymbol{n}_1, \tag{2}$$

$$\boldsymbol{X} = \boldsymbol{B}_2 + \boldsymbol{R}_{\beta 2} z_2 \boldsymbol{e}_1 + l_2 \boldsymbol{n}_2. \tag{3}$$

where $\boldsymbol{e}_1 = (0 \;\; 1)^{\mathrm{T}}$, $\boldsymbol{B}_1 = (-D/2 \;\; 0)^{\mathrm{T}}$, $\boldsymbol{B}_2 = (D/2 \;\; 0)^{\mathrm{T}}$, $\boldsymbol{R}_{\beta i} = \begin{pmatrix} \cos\beta_i & -\sin\beta_i \\ \sin\beta_i & \cos\beta_i \end{pmatrix}$, for $i = 1,2$.

When tiny parameter errors are considered, Eq. (2) can be expressed as

$$\begin{aligned} \boldsymbol{X} + \delta\boldsymbol{X} = {} & \boldsymbol{B}_1 + \delta\boldsymbol{B}_1 + (\boldsymbol{R}_{\beta 1} + \delta\boldsymbol{R}_{\beta 1})(z_1 + \delta z_1)\boldsymbol{e}_1 \\ & + (l_1 + \delta l_1)(\boldsymbol{n}_1 + \delta\boldsymbol{n}_1). \end{aligned} \tag{4}$$

where $\delta\boldsymbol{R}_{\beta 1} = \delta\beta_1 \boldsymbol{W}\boldsymbol{R}_{\beta 1}$, $\boldsymbol{W} = \begin{pmatrix} 0 & -1 \\ 1 & 0 \end{pmatrix}$.

Eq. (3) becomes

$$\begin{aligned} \boldsymbol{X} + \delta\boldsymbol{X} = {} & \boldsymbol{B}_2 + \delta\boldsymbol{B}_2 + (\boldsymbol{R}_{\beta 2} + \delta\boldsymbol{R}_{\beta 2})(z_2 + \delta z_2)\boldsymbol{e}_1 \\ & + (l_2 + \delta l_2)(\boldsymbol{n}_2 + \delta\boldsymbol{n}_2). \end{aligned} \tag{5}$$

where $\delta\boldsymbol{R}_{\beta 2} = \delta\beta_2 \boldsymbol{W}\boldsymbol{R}_{\beta 2}$, $\mathbf{W} = \begin{pmatrix} 0 & -1 \\ 1 & 0 \end{pmatrix}$.

Subtracting Eq. (2) from Eq. (4), and ignoring the second and higher products, we can obtain

$$\delta\boldsymbol{X} = \delta\boldsymbol{B}_1 + \delta\beta_1 \boldsymbol{W}\boldsymbol{R}_{\beta 1} z_1 \boldsymbol{e}_1 + \delta z_1 \boldsymbol{R}_{\beta 1}\boldsymbol{e}_1 + \delta l_1 \boldsymbol{n}_1 + l_1 \delta\boldsymbol{n}_1. \tag{6}$$

Subtracting Eq. (3) from Eq. (5), and ignoring the second and higher products, we can obtain

$$\delta\boldsymbol{X} = \delta\boldsymbol{B}_2 + \delta\beta_2 \boldsymbol{W}\boldsymbol{R}_{\beta 2} z_2 \boldsymbol{e}_1 + \delta z_2 \boldsymbol{R}_{\beta 2}\boldsymbol{e}_1 + \delta l_2 \boldsymbol{n}_2 + l_2 \delta\boldsymbol{n}_2. \tag{7}$$

Multiplying both sides of Eq. (6) by $\boldsymbol{n}_1^{\mathrm{T}}$ and using $\boldsymbol{n}_1^{\mathrm{T}}\boldsymbol{n}_1 = 1$, $\boldsymbol{n}_1 \delta\boldsymbol{n}_1 = 0$, lead to

$$\boldsymbol{n}_1^{\mathrm{T}}\delta\boldsymbol{X} = \boldsymbol{n}_1^{\mathrm{T}}\delta\boldsymbol{B}_1 + \boldsymbol{n}_1^{\mathrm{T}}\boldsymbol{W}\boldsymbol{R}_{\beta 1} z_1 \boldsymbol{e}_1 \delta\beta_1 + \boldsymbol{n}_1^{\mathrm{T}}\boldsymbol{R}_{\beta 1}\boldsymbol{e}_1 \delta z_1 + \delta l_1. \tag{8}$$

Multiplying both sides of Eq. (7) by $\boldsymbol{n}_2^{\mathrm{T}}$ and using $\boldsymbol{n}_2^{\mathrm{T}}\boldsymbol{n}_2 = 1$, $\boldsymbol{n}_2 \delta\boldsymbol{n}_2 = 0$, lead to

$$\boldsymbol{n}_2^{\mathrm{T}}\delta\boldsymbol{X} = \boldsymbol{n}_2^{\mathrm{T}}\delta\boldsymbol{B}_2 + \boldsymbol{n}_2^{\mathrm{T}}\boldsymbol{W}\boldsymbol{R}_{\beta 2} z_2 \boldsymbol{e}_1 \delta\beta_2 + \boldsymbol{n}_2^{\mathrm{T}}\boldsymbol{R}_{\beta 2}\boldsymbol{e}_1 \delta z_2 + \delta l_2. \tag{9}$$

Rewrite Eqs. (8) and (9) in a matrix form

$$\begin{aligned} \begin{pmatrix} \boldsymbol{n}_1^{\mathrm{T}} \\ \boldsymbol{n}_2^{\mathrm{T}} \end{pmatrix} \begin{pmatrix} \delta y \\ \delta z \end{pmatrix} = {} & \begin{pmatrix} -\boldsymbol{n}_{1(1)}^{\mathrm{T}}/2 & \boldsymbol{n}_1^{\mathrm{T}}\boldsymbol{R}_{\beta 1}\boldsymbol{e}_1 & 0 \\ \boldsymbol{n}_{2(1)}^{\mathrm{T}}/2 & 0 & \boldsymbol{n}_2^{\mathrm{T}}\boldsymbol{R}_{\beta 2}\boldsymbol{e}_1 \end{pmatrix} \begin{pmatrix} \delta D \\ \delta z_1 \\ \delta z_2 \end{pmatrix} \\ & + \begin{pmatrix} 1 & 0 \\ 0 & 1 \end{pmatrix} \begin{pmatrix} \delta l_1 \\ \delta l_2 \end{pmatrix} + \begin{pmatrix} \boldsymbol{n}_1^{\mathrm{T}}\boldsymbol{W}\boldsymbol{R}_{\beta 1}\boldsymbol{e}_1 z_1 & 0 \\ 0 & \boldsymbol{n}_2^{\mathrm{T}}\boldsymbol{W}\boldsymbol{R}_{\beta 2}\boldsymbol{e}_1 z_2 \end{pmatrix} \begin{pmatrix} \delta\beta_1 \\ \delta\beta_2 \end{pmatrix}. \end{aligned} \tag{10}$$

where $\boldsymbol{n}_{i(1)}^{\mathrm{T}}$ $(i = 1,2)$ is first component of $\boldsymbol{n}_i^{\mathrm{T}}$.

Then the posture error of the platform can be formulated as

$$\begin{aligned} \begin{pmatrix} \delta y \\ \delta z \end{pmatrix} = {} & \begin{pmatrix} \boldsymbol{n}_1^{\mathrm{T}} \\ \boldsymbol{n}_2^{\mathrm{T}} \end{pmatrix}^{-1} \begin{pmatrix} -\boldsymbol{n}_{1(1)}^{\mathrm{T}}/2 & \boldsymbol{n}_1^{\mathrm{T}}\boldsymbol{R}_{\beta 1}\boldsymbol{e}_1 & 0 \\ \boldsymbol{n}_{2(1)}^{\mathrm{T}}/2 & 0 & \boldsymbol{n}_2^{\mathrm{T}}\boldsymbol{R}_{\beta 2}\boldsymbol{e}_1 \end{pmatrix} \begin{pmatrix} \delta D \\ \delta z_1 \\ \delta z_2 \end{pmatrix} \\ & + \begin{pmatrix} \boldsymbol{n}_1^{\mathrm{T}} \\ \boldsymbol{n}_2^{\mathrm{T}} \end{pmatrix}^{-1} \begin{pmatrix} 1 & 0 \\ 0 & 1 \end{pmatrix} \begin{pmatrix} \delta l_1 \\ \delta l_2 \end{pmatrix} \\ & + \begin{pmatrix} \boldsymbol{n}_1^{\mathrm{T}} \\ \boldsymbol{n}_2^{\mathrm{T}} \end{pmatrix}^{-1} \begin{pmatrix} \boldsymbol{n}_1^{\mathrm{T}}\boldsymbol{W}\boldsymbol{R}_{\beta 1}\boldsymbol{e}_1 z_1 & 0 \\ 0 & \boldsymbol{n}_2^{\mathrm{T}}\boldsymbol{W}\boldsymbol{R}_{\beta 2}\boldsymbol{e}_1 z_2 \end{pmatrix} \begin{pmatrix} \delta\beta_1 \\ \delta\beta_2 \end{pmatrix}. \end{aligned} \tag{11}$$

At pose *i*, Eq. (11) can be rewritten as

$$(\delta\boldsymbol{X}_i)_{2\times 1} = (\boldsymbol{J}_i)_{2\times 7}(\delta\boldsymbol{p})_{7\times 1}. \tag{12}$$

where $\delta\boldsymbol{X}_i = (\delta y_i \;\; \delta z_i)^{\mathrm{T}}$ is the posture error of end-effector at pose *i*, $\boldsymbol{p} = (D \;\; z_1 \;\; z_2 \;\; l_1 \;\; l_2 \;\; \beta_1 \;\; \beta_2)^{\mathrm{T}}$, $\boldsymbol{J}_i$

is the Jacobian matrix connecting pose error $\delta \boldsymbol{X}_i$ with parameter errors $\delta \boldsymbol{p}$.

2.3 Identification analysis based on the MLCs

The four theorems of the MLCs in identification proposed by Ref. [10] offer a powerful support for identification analysis. Through analyzing the columns of the square upper triangular matrix $\boldsymbol{R}$ which is generated by QR decomposition of the identification matrix, the four theorems of the MLCs are obtained: (1) if there exist zero column vectors in $\boldsymbol{R}$, then the error parameters corresponding to the zero column vectors of $\boldsymbol{R}$ are unidentifiable; (2) if there exist proportional column vectors in $\boldsymbol{R}$, then only one linear combination, which is formed by the error parameters corresponding to the proportional column vectors of $\boldsymbol{R}$, can be identified; (3) if there exist linear dependent column vectors in $\boldsymbol{R}$, then only n linear combination (n is the number of column vectors which form the maximal linearly independent subset of the linear dependent column vectors), which is formed by the error parameters corresponding to the linear dependent column vectors of $\boldsymbol{R}$, can be identified; and (4) The number of linear combinations of the error parameters is the rank of $\boldsymbol{R}$. Thus, the identification analysis is completed, and the MLCs of error parameters can be found.

2.3.1 Identification analysis in RM

There is no nominal orientation change in the movement of the parallel manipulator, the difference between absolute precision and relative precision is a constant offset[12], and cannot influence shape precision while machining. Then only relative precision should be considered in precision evaluation.

In calibration, only relative output information should be measured. Through identification and error compensation, only relative precision will be improved, and this can meet engineering requirement.

When only relative precision is considered, Eq. (12) can be rewritten as

$$\delta \boldsymbol{X}_i - \delta \boldsymbol{X}_0 = (\boldsymbol{J}_i - \boldsymbol{J}_0)\delta \boldsymbol{p} . \tag{13}$$

Where $\boldsymbol{J}_0$ and $\delta \mathbf{X}_0$ are the Jacobian matrix and the posture error at the reference configuration 0, respectively.

In the whole workspace of the parallel manipulator, totally 101 configurations are selected randomly and on each configuration all two components of $\boldsymbol{X}$ are used. One configuration 0 is regarded as the reference configuration 0, and the Jacobian matrix $\boldsymbol{J}_0$ can be obtained from Eq. (12). Similarly, on other configurations i, and $\boldsymbol{J}_i$, for $i = 1,2,\cdots,100$ can be obtained. According to Eq. (13), the aggregated relative identification matrix $\boldsymbol{W}$ can be written as

$$\boldsymbol{W}_{200\times 7} = \begin{pmatrix} \boldsymbol{J}_1 - \boldsymbol{J}_0 \\ \boldsymbol{J}_2 - \boldsymbol{J}_0 \\ \vdots \\ \boldsymbol{J}_{100} - \boldsymbol{J}_0 \end{pmatrix} . \tag{14}$$

Analyzing the identification of $\boldsymbol{W}$ by using the four theorems of the MLCs, a set of MLCs of error parameters in RM can be obtained as

$$\boldsymbol{p}_{\mathrm{r}} = \begin{pmatrix} D & z_1 - z_2 & l_1 & l_2 & \beta_1 & \beta_2 \end{pmatrix}^{\mathrm{T}} . \tag{15}$$

The relative precision of the parallel manipulator is determined by these 6 MLCs of error parameters, that is to say, the 6 MLCs can be identified in calibration of RM.

According to the results of identification analysis, the corresponding column of z_2 in $(\boldsymbol{J}_i - \boldsymbol{J}_0)$ is eliminated, then $(\boldsymbol{J}_i - \boldsymbol{J}_0)$ is changed to $(\boldsymbol{J}_{i\mathrm{r}} - \boldsymbol{J}_{0\mathrm{r}})$, and Eq. (13) can be rewritten as

$$\delta \boldsymbol{X}_i - \delta \boldsymbol{X}_0 = (\boldsymbol{J}_{i\mathrm{r}} - \boldsymbol{J}_{0\mathrm{r}})\delta \boldsymbol{p}_{\mathrm{r}} . \tag{16}$$

2.3.2 General RM in practice

Considering actual motion of the parallel manipulator, four kinds of RMs are developed, as follows:

RM 1: Fixing the nominal value of the coordinate z and letting the end-effector move along the y-axis, measure the δy for the reference plane parallel to the $O_B - xz$ plane by using a laser interferometer.

RM 2: Fixing the nominal value of the coordinate y and letting the end-effector move along the z-axis, measure the δz for the reference plane parallel to the $O_B - xy$ plane by using a laser interferometer.

RM 3: Fixing the nominal value of the coordinate z and letting the end-effector move along the y-axis, measure the δz for the reference plane parallel to the $O_B - xy$ plane by using a micrometer.

RM 4: Fixing the nominal value of the coordinate y and letting the end-effector move along the z-axis, measure the δy for the reference plane perpendicular to the y-axis by using a micrometer.

The sketches of RMs 1-4 are shown in Fig. 3.

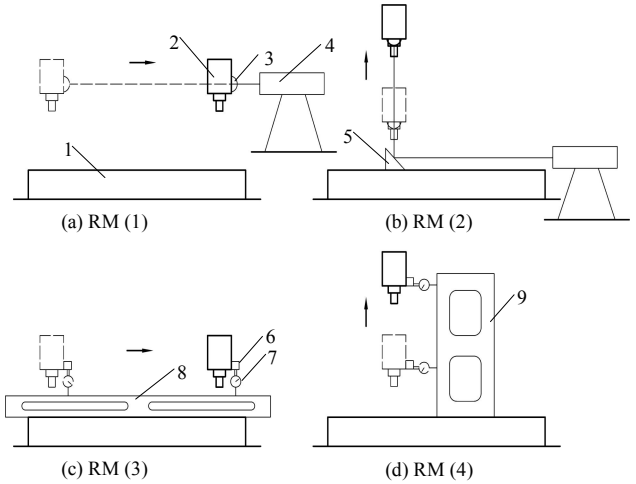

1. Worktable 2. Platform 3. Reflector 4. Laser interferometer 5. Prism 6. Fixture 7. Micrometer 8. Parallel ruler 9. Vertical ruler

Fig. 3. Sketches of RMs 1-4

2.3.3 Identification analysis of each RM

The identification analysis of each RM is based on the MLCs.

In RM 1, there are three horizontal measurement lines, including $z=0,750,1500$ mm , 11 configurations are chosen, whose y values are $-1500,-1200,-900,\cdots,1500$ mm , respectively. In these configurations, $(0,0)$, $(0,750)$ and $(0,1500)$ are regarded as reference configurations on each measurement line. Since only δy is measured, the first row of $(\boldsymbol{J}_{ir}-\boldsymbol{J}_{0r})$ in Eq. (16) is used. An aggregated relative identification matrix like $\boldsymbol{W}$ in Eq. (16) is obtained. According to identification analysis, δD , δl_1 , δl_2 , $\delta\beta_1+(\delta z_1-\delta z_2)/D$ and $\delta\beta_2+(\delta z_1-\delta z_2)/D$ can be identified.

There are three vertical measurement lines in RM 2, including $y=-1500,0,1500$ mm . 6 configurations are selected on each measurement line, whose z values are $0,300,600,\cdots,1500$ mm respectively. $(-1500,0)$, $(0,0)$ and $(1500,0)$ are regarded as reference configurations of each measurement line. Since δz is measured, an aggregated relative identification matrix is formed by the second row of $(\boldsymbol{J}_{ir}-\boldsymbol{J}_{0r})$. Through identification analysis, only $\delta\beta_1-\delta\beta_2$ can be identified.

RM 3 has the same measurement configurations and reference configurations as RM 1. δz is measured and an aggregated relative identification matrix is formed by the second row of $(\boldsymbol{J}_{ir}-\boldsymbol{J}_{0r})$. According to identification analysis, δD , $\delta z_1-\delta z_2$, δl_1 , δl_2 , $\delta\beta_1$ and $\delta\beta_2$ can be identified.

RM 4 has the same measurement configurations and reference configurations as RM 2. δy is measured and an aggregated relative identification matrix is formed by the first row of $(\boldsymbol{J}_{ir}-\boldsymbol{J}_{0r})$. According to identification analysis, $\delta\beta_1$ and $\delta\beta_2$ can be identified.

2.4 Determination of a step measurement

By comparing the identified MLCs of each measurement mentioned above, some conclusions can be drawn.

The identified MLCs in RM 4 contain those in RM 2. In order to compare their observability, a noise amplification index[13] is introduced

$$\boldsymbol{O}=\frac{\sqrt[L]{\prod_{i=1}^{L}\sigma_i}}{\sqrt{m}}. \tag{17}$$

where m is the number of measurement poses, L is the number of singular values, and σ_i , $i=1,2,\cdots,L$, are the singular values of the identification matrix.

Based on Eq. (17), it can be seen that the observability in RM 4 is stronger than that in RM 2. Further, since it is difficult for the measurement instruments in RM 2 to be adjusted, RM 2 is excluded.

The identified MLCs in RM 3 contain those in RM 4, but the observability in RM 4 is stronger than that in RM 3, so RM 4 is reserved.

On the basis of that different MLCs can be identified in different measurements, in the calibration process, measurements can be implemented step by step, identification and error compensation can also be carried out step by step: Firstly, identify the MLCs $\delta\beta_1$ and $\delta\beta_2$ by using RM 4. Secondly, use RM 1 or RM 3 to identify four MLCs δD , $\delta z_1-\delta z_2$, δl_1 and δl_2 . But in order to enhance the observability, in-depth analysis is needed.

Through observation, RM 1 and RM 3 can be carried out easily at the same time in practice. Define this kind of measurement as RM 5, which has the same measurement configurations and reference configurations as RM 1. Both δy and δz are measured and an aggregated relative identification matrix is formed by the first and second rows of $(\boldsymbol{J}_{ir}-\boldsymbol{J}_{0r})$. According to identification analysis, δD , $\delta z_1-\delta z_2$, δl_1 , δl_2 , $\delta\beta_1$ and $\delta\beta_2$ can be identified.

In order to compare the observability of identified MLCs in RM 1, 3 and 5, the same measurement configurations and reference configurations as RM1 are selected in these RMs. The corresponding aggregated relative identification matrixes for the MLCs δD , $\delta z_1-\delta z_2$, δl_1 and δl_2 are formed, respectively. Through calculating the noise amplification index, it can be seen that the observability in RM 5 is stronger than that in RM 1 and RM 3, so RM 5 is selected to identify the four MLCs, i.e. δD , $\delta z_1-\delta z_2$, δl_1 and δl_2 .

As a result, both measurement costs and observability are considered, a step measurement can be determined:

Step 1: Identify $\delta\beta_1$ and $\delta\beta_2$ by using RM 4.

Step 2: Identify δD , $\delta z_1-\delta z_2$, δl_1 and δl_2 by using RM 5.

2.4.1 Pose Determination

After determining the step measurement, optimal poses of each step measurement are obtained through calculating

the noise amplification index: In step 1, there are two vertical measurement lines, including $y=-1500,1500$ mm . Two configurations are selected, whose z values are $0,900$ mm , respectively. $(-1500,0)$ and $(1500,0)$ are regarded as reference configurations on each measurement line. In step 2, three configurations are chosen, whose y values are $-1500,0,1500$ mm , respectively, and $z=200$ mm , and the reference configuration is $(0,200)$.

2.5 Step error compensation

In step 1, when $(\delta\beta_1)_e$ and $(\delta\beta_2)_e$ are estimated, update $\beta_1=\beta_1+(\delta\beta_1)_e$ and $\beta_2=\beta_2+(\delta\beta_2)_e$ in the control system, then correct the new home position of the actuators. Repeat this step until the relative y direction errors of the selected poses are sufficiently small.

In step 2, when $(\delta D)_e$, $(\delta z_1-\delta z_2)_e$, $(\delta l_1)_e$ and $(\delta l_2)_e$ are estimated, update $\delta D=(\delta D)_e$, $\delta l_1=(\delta l_1)_e$ and $\delta l_2=(\delta l_2)_e$ in the control system, then correct the new home position of the actuators through the inverse kinematics, and the home position of the actuator z_1 should be updated as $z_1=z_1-(\delta z_1-\delta z_2)_e$. Repeat this step until the relative y and z direction errors of the selected poses are sufficiently small.

3 Linear Forecast Real-time Error Compensation

Due to large working space, heavy-duty and over-constrained mechanism, the values of some geometrical parameters change little at different pose, then the end-effector positioning accuracy is affected by the tiny changes of the parameters. But the errors of the variable parameters can not compensated by kinematic calibration. Therefore, a linear forecast real-time error compensation is developed to enhance the precision of the end-effector.

In the linear forecast real-time error compensation:

Firstly, mesh grid in the working space according to the grade of the changes of the end-effector errors. When the end-effector errors change rapidly, the mesh is divided densely; when the end-effector errors change slowly, the mesh is divided sparsely.

Secondly, measure the end-effector errors by measuring instruments in the node of grid.

Thirdly, in the numerical control program, save the error values measured by measuring instruments in the form of array.

Finally, the configuration, where the drivers of control system are reset to their home positions, is set as the reference configuration 0 of the whole workspace. Relative error $\delta\boldsymbol{X}_i-\delta\boldsymbol{X}_0$ on a configuration i relative to the configuration 0 can be figured out by linear interpolation between the neighboring array element values. Command $\boldsymbol{X}_i$ is compensated before it is set to the drivers by $\delta\boldsymbol{X}_i-\delta\boldsymbol{X}_0$, then $\boldsymbol{X}_i'=\boldsymbol{X}_i-(\delta\boldsymbol{X}_i-\delta\boldsymbol{X}_0)$ is used as new command to control the drives. The processor is shown in Fig. 4.

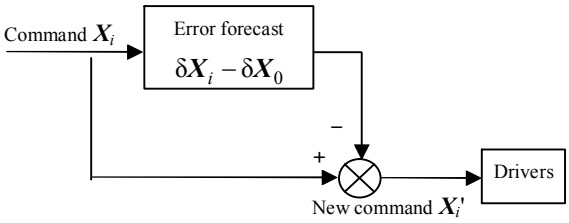

Fig.4. Forecast real-time error compensation processor

The linear forecast real-time error compensation process is a linear simplification, and both its precision and efficiency are good.

4 Experimental Results

Before calibration, the deviations along y and z are about in a range of ±1.589 mm and ±1.715 mm , respectively. According to the step measurement in section 2.4, identification by least square method, and step error compensation in section 2.5, a practical experiment of the step calibration is carried out.

Finally, the detailed results of the step calibration are shown in Fig. 5.

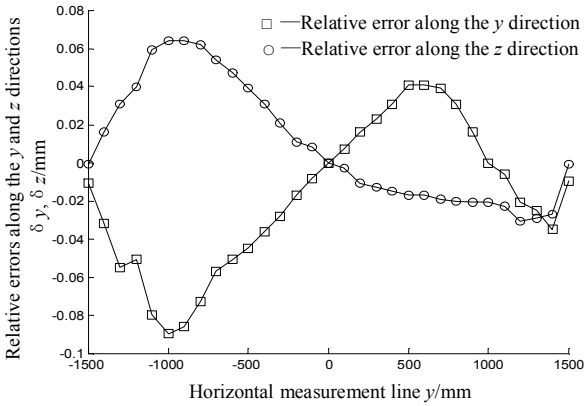

Fig. 5. Relative errors along the y and z directions of horizontal line after calibration

On the horizontal lines, deviations along y and z are measured at the same time. The deviations after calibration are in a range of ±0.07 mm and ±0.05 mm , respectively. The relative precision of the parallel manipulator has been improved, but this cannot meet the demand of machining accuracy.

By analyzing, the characters with large working space, heavy-duty and over-constrained mechanism produce small deformation in the 2-DOF planar parallel manipulator. The values of some geometrical parameters change little at the different pose. These variable parameters cannot be compensated by kinematic calibration. In order to further improve the relative precision of the parallel manipulator, the linear forecast real-time error compensation is carried

out. The results of the forecast error compensation are shown in Fig. 6.

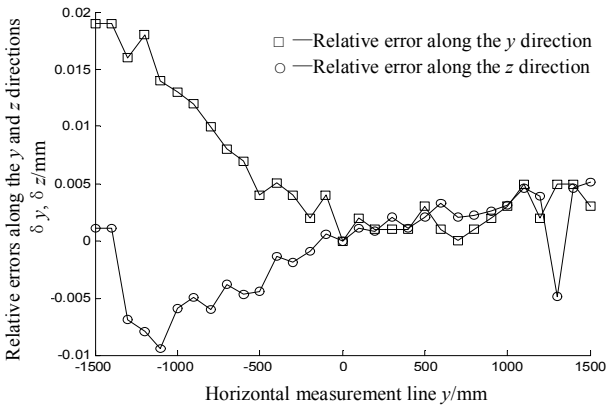

Fig. 6. Relative errors along the y and z directions of horizontal line after linear forecast real-time error compensation

From Fig. 6, after the linear forecast real-time error compensation, the relative precision of the parallel manipulator has been improved to ± 0.01 mm, from ± 0.07 mm and ± 0.05 mm after calibration. The final precision of the parallel manipulator has come close to measurement precision and its repeatability. Experiment results prove that the proposed method combined kinematic calibration and linear forecast real-time error compensation is effective and feasible.

5 Conclusions

(1) A method has been proposed to improve the accuracy of a 2-DOF planar parallel manipulator of a hybrid machine tool, which is characterized with large working space, heavy-duty and over-constrained mechanism.

(2) The method combined step kinematic calibration and linear forecast real-time error compensation, the end-effector errors caused by the errors of major constant geometrical parameters is compensated in the step kinematic calibration, and the linear forecast real-time error compensation is used to compensate the end-effector errors caused by other parameters after the kinematic calibration.

(3) The method take the advantages of the step kinematic calibration and the linear forecast real-time error compensation, hence the method is fast, convenient and effective.

(4) The experiment is performed to verify the effectiveness of the proposed method.

References

[1] Gromann K, Kauschinger B, Szatmári S. Kinematic calibration of a hexapod of simple design[J]. Production Engineering, 2008, 2(3): 317-325.

[2] Chiu Y J, Perng M H. Self-calibration of a general hexapod manipulator using cylinder constraints[J]. International Journal of Machine Tools and Manufacture, 2003, 43(10): 1 051-1 066.

[3] Huang Tian, Chetwynd D G, Whitehouse D J, et al. A general and novel approach for parameter identification of 6-DOF parallel kinematic machines[J]. Mechanism and Machine Theory. 2005, 40(2): 219-239.

[4] Meggiolaro M A, Dubowsky S. An analytical method to eliminate the redundant parameters in robot calibration[C]//Proceedings of the 2000 IEEE International Conference on Robotics & Automation, San Francisco, 2000: 3 609-3 615.

[5] Osamu S, Ken S, Ryoshu F, et al. Artefact calibration of parallel mechanism, kinematic calibration with a priori knowledge[J]. Measurement Science and Technology, 2004, 15(6): 1 158-1 165.

[6] Abtahi M, Pendar H, Alasty A, et al. Calibration of parallel kinematic machine tools using mobility constraint on the tool center point[J]. International Journal of Advanced Manufacturing Technology, 2009,45(5-6): 531-539.

[7] Besnard S, Khalil W. Calibration of parallel robots using two inclinometers[C]//Proceedings of IEEE International Conference on Robotics and Automation, Detroit, 1999: 1 758-1 763.

[8] David D, Emiris I Z. Robust parallel robot calibration with partial information[C]//Proceedings of ICRA, Seoul, 2001: 3 262-3 267.

[9] Huang Tian, Tang Guo Bao, Li Si Wei, et al. Kinematic calibration of a class of parallel kinematic machines(PKM) with fewer than six degrees of freedom[J]. Science in China Series E, 2003, 46(5): 515-526.

[10] Chang Peng, Li Tie Min, Guan Li Wen. Minimal linear combinations of the error parameters for kinematic calibration of parallel kinematic machines[C]//Proceedings – 5th Chemitz Parallel Kinematics Seminar, Chemnitz, Germany, 2006: 565-583.

[11] Wu Jun, Wang Jin Song, Li Tie Min, et al. Dynamic analysis of the 2-DOF planar parallel manipulator of a heavy duty hybrid machine tool[J]. International Journal of Advanced Manufacturing Technology, 2007, 34(3-4): 413-420.

[12] Patel A J, Ehmann K F. Calibration of a hexapod machine tool using a redundant leg[J]. International Journal of Machine Tools and Manufacture, 2000, 40(4): 489-512.

[13] BORM J H, MENQ C H. Determination of optimal measurement configurations for robot calibration based on observability measure[J]. International Journal of Robotics Research, 1991, 10(1): 51-63.

Biographical notes

CHANG Peng, born in 1980, is currently a Postdoctoral Researcher in Hi-tech Innovation Center, Institute of Automation Chinese Academy of Sciences, Beijing, China. He received the B.S. and Ph.D. degrees in mechanical engineering from Tsinghua University, Beijing, China, in 2002 and 2008. His research interests include accuracy analysis and kinematic calibration of parallel kinematic machines, and design of intelligent robotics.
Tel: +86-10-62638825; E-mail: changpeng@tsinghua.org.cn

LI Chengrong, born in 1961, Ph.D. is currently a professor in Hi-tech Innovation Center, Institute of Automation Chinese Academy of Sciences, Beijing, China. His research interests include intelligent robotics and speech recognition.
E-mail: lich@hitic.ia.ac.cn

LI Tiemin, born in 1971, Ph.D. is currently an associate professor in the Department of Precision Instruments and Mechanology, Tsinghua University, Beijing, China. His research interests include parallel kinematic machines and redundant parallel mechanisms.
E-mail: litm@tsinghua.edu.cn